Host(beta zeolite)–guest (copper(II)–methyladenine complex) nanomaterials: synthesis and characterization†

Catarina Teixeira,[a] Paolo Pescarmona,[b] M. Alice Carvalho,[a] António M. Fonseca*[a] and Isabel C. Neves*[a]

Received (in Montpellier, France) 9th May 2008, Accepted 21st July 2008
First published as an Advance Article on the web 17th September 2008
DOI: 10.1039/b807904h

The guest copper(II)–methyladenine complex was entrapped into beta zeolite (BEA) as a host by a process of sequential introduction of the components in the liquid phase followed by assembly inside the void space of the zeolite. The beta zeolite was prepared by an original technique. The appropriate process chosen for the *in situ* complex synthesis was using a 9-methyladenine ligand : copper(II) molar ratio of 4 : 1. The new host–guest nanomaterial was purified by Soxhlet extraction. The BEA zeolite with copper(II)–methyladenine complex was characterized by several techniques: SEM and XRD, chemical analysis (CA), spectroscopic methods (EPR, FTIR, UV-Vis and XPS) and TGA (thermal analysis). Analysis of the data indicates that the guest copper(II) complex was effectively immobilized in BEA without any modification of the morphology and structure of the zeolite. The coordination of the 9-methyladenine ligand with copper(II) ion as guest in the host nanomaterial was obtained with a preferential 1 : 1 stoichiometry.

1 Introduction

Zeolites find broad application in heterogeneous catalysis and also attract interest in materials science for the development of functional materials.[1,2] Zeolites present a crystalline structure in which active compounds can be included. In addition to the space constraints imposed by the zeolite, the negative charge of the zeolite framework and the distribution of the positive charges of the cations can lead to specific interactions with the included compound, which in turn induce structural and functional modification in the active compound as compared to its behavior as free species in solution.[2]

The heterogenization of a functional guest inside the zeolites preventing the diffusion of the particle out of the solid framework is very promising for application in catalysis.[2–9] The host material supplies additional stability to the incorporated active center, thereby expanding the physical and chemical resistance of the catalyst. These new host–guest nanomaterials are interesting for application as biomimetic heterogeneous catalysts for the oxidation of alkanes, alkenes and alcohols.[10–12]

However, the use of zeolites as hosts for metal complexes has been mainly restricted to faujasite-type zeolites,[9–15] with few examples from other zeolites structures, such as mordenite and EMT.[16,17] Work in this field with beta zeolite (BEA) are limited, despite this material being known for several years[18,19] and presenting a structure appropriate to act as a solid matrix in the immobilization of chemical species.

In contrast with zeolite Y, beta zeolite does not present supercages but a tridimensional array of intersecting channels with 12-membered ring apertures with a diameter of 7.6 Å.[20] The intersection of two perpendicular channels defines oval cavities (7.4 × 11 Å), which present a suitable size for hosting transition metal complexes.

Zeolite BEA can be prepared in the form of nanoparticles with a diameter of around 30 nm. The use of nanosized beta zeolite as host material for metal complexes can prove advantageous in many respects.

Generally, host–guest materials present a higher concentration of guests in the zone closer to the external surface of the host, due to the diffusion rate of the guest precursors (*i.e.* the ligands) through the porous structure during the synthesis of the host–guest material. The use of smaller host particles would intrinsically reduce this gradient of concentration, thus allowing a higher loading of guest per gram of host. Moreover, when large zeolite particles are used, guest compounds located in the inner part of the host material are not easily accessible for catalytic reactions. This limitation can be overcome using zeolite nanoparticles, in which a larger fraction of the hosting cavities is located close to the external surface.

It has been shown that Y-zeolite encapsulated transition metal complexes exhibit good catalytic activity in the oxidation of alcohols and alkenes with peroxide at relatively low temperatures.[4,9,21,22] The first results with copper(II)–amino acid complexes [$Cu(AA)_n^{m+}$] were obtained by Weckhuysen *et al.*[21,22] by encapsulation in Y-zeolite through ion-exchange from aqueous solutions containing both the amino acid (AA) and copper(II), with an AA : Cu(II) ratio of 5 : 1.

Inspired by this work, copper(II)–purine complexes encaged in zeolite Y were studied and their catalytic potential was demonstrated for the cyclohexene oxidation reaction in the presence of the *tert*-butyl hydroperoxide (*t*-BuOOH) as the oxygen source.[9]

[a] *Departamento de Química, Centro de Química, Universidade do Minho, Campus de Gualtar, 4710-057 Braga, Portugal. E-mail: amcf@quimica.uminho. E-mail: ineves@quimica.uminho.pt*
[b] *Centre for Surface Chemistry and Catalysis, K.U. Leuven, Kasteelpark Arenberg 23, 3001 Heverlee, Belgium*

† Electronic supplementary information (ESI) available: Thermogravimetric data. See DOI: 10.1039/b807904h

This work explores the possibility of the immobilization of the copper(II)–methyladenine complex as guest in the void space of the host beta zeolite nanoparticles. The synthesis and the characterization of the new host–guest nanomaterial includes: (i) the preparation of Cu-exchanged NaBEA and of the 9-methyladenine ligand and (ii) the synthesis of the immobilized complex. The ion-exchange procedure was followed by the *in situ* synthesis of the encapsulated metal complex in the BEA zeolite with a ligand : Cu(II) molar ratio of 4 : 1. The 9-methyladenine ligand diffused into the beta zeolite framework and chelated with the previously exchanged transition copper ion. The formed complex is unable to escape from the host zeolite due to its much larger size than the zeolite pore diameter.[5] The obtained host–guest nanomaterial was fully characterised by chemical analysis (CA), spectroscopic methods (EPR, FTIR and UV-Vis), powder X-ray diffraction (XRD), scanning electron microscopy (SEM) and thermal analysis (TGA).

2 Experimental

2.1 Methods

2.1.1 Synthesis of the NaBEA. The NaBEA with Si/Al atomic ratio = 9 was synthesized according to a previously published procedure.[23] 39.3 g (0.654 mol) of SiO_2 silica gel Cab-o-sil M-5 were slowly added to 171.3 g of tetraethylammonium hydroxide (TEAOH) 35 wt% in H_2O (0.407 mol of TEAOH), while stirring: a white gel was obtained. A solution of 4.89 g (5.97×10^{-2} mol) of $NaAlO_2$ dissolved in 69.3 mL of deionised H_2O was added to the gel while stirring and manually mixing: a thicker gel was obtained. Upon mixing and aging, the gel became more fluid. The gel was stirred for 2 h and then transferred into Teflon-lined stainless-steel autoclaves. The autoclaves were closed and heated statically to 150 °C in an oven. After 6 days at 150 °C, the autoclaves were removed from the oven and allowed to cool to room temperature. The white–yellow gel-like precipitate was separated from the supernatant by centrifugation (4000 rpm, 15 min.). Next, the solid was washed repeatedly with H_2O until the washing had a pH < 9. The white sample was dried in an oven at 110 °C for 12 h (final yield: 29.15 g). Finally, the sample was calcined at 600 °C for 10 h (30 to 600 °C at 1 °C min^{-1}). Powder XRD showed that the sample consisted of highly crystalline pure beta zeolite. The sample was characterised by SEM, EDX and ICP-OES elemental analyses.

2.1.2 Synthesis of 9-methyladenine ligand. 9-Methyladenine was synthesised using a procedure previously reported by Ramsden and co-workers.[24] The starting material was 5-amino-4-cyano-*N*-methylimidazole **1**[25] which was reacted with triethyl orthoformate followed by treatment with ammonia gas (Scheme 1).

The imidazole **1** (0.78 g, 6.36 mmol), triethyl orthoformate (4.2 mL, 25.44 mmol) and acetic anhydride (2.4 mL, 25.44 mmol) were refluxed until TLC showed absence of starting material. The reaction mixture was concentrated under vacuum and *n*-hexane was added to the residue. After cooling for 30 min, an off-white solid was filtered off, washed with diethyl ether and identified by spectroscopic and analytic

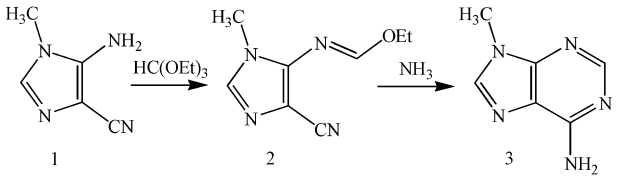

Scheme 1 Synthesis of the 9-methyladenine ligand.

method as the iminoether imidazole, compound **2** (0.50 g, 3.01 mmol, 47% yield).

The iminoether imidazole **2** (0.48 g, 2.89 mmol) was suspended in methanol (1.0 mL), under magnetic stirring, at 0 °C. Ammonia gas was bubbled through the suspension for 15 min and the reaction was completed after a further 45 min, as evidenced by TLC. The excess of ammonia was eliminated under vacuum, cold methanol was added to the residue and the off-white solid was filtered off and washed with cold methanol. The isolated solid **3** was identified as 9-methyladenine (0.35 g, 2.35 mmol, 87% yield); mp = 310 °C (lit.[26] = 310 °C).

2.1.3 Immobilization of the guest. The immobilization process was based on a previous established procedure with a molar ratio ligand : Cu(II) = 4 : 1.[9] The experimental procedure starts with the cation exchange of NaBEA zeolite: an aqueous solution containing 3.73×10^{-1} mmol of $Cu(NO_3)_2 \cdot 3H_2O$ was added to 1.0 g of zeolite (previously dried at 150 °C during 12 h). The resulting mixture was stirred for 12 h at room temperature. The light blue suspension was filtered off and dried in an oven at 60 °C for 12 h and finally dried in vacuum for 2 h (Cu–NaBEA). A solution of the 9-methyladenine ligand (1.49 mmol) in 50 mL of distilled water was added to the Cu–NaBEA. The suspension was stirred for 24 h at room temperature, until the brown–green colored aqueous solution became colorless, indicating that the methyladenine ligand was adsorbed by the zeolite. The pH of the synthesis mixture was continuously monitored at 7.0. Next, the suspension was filtered off, in order to remove the excess of methyladenine ligand. The grey solid was washed with distilled water and dried at 60 °C for 8 h.

The excess or not coordinated ligand, as well as the residual metal complex physically adsorbed on the external surface of the zeolite was removed by Soxhlet extraction with ethanol for 6 h. Finally, the host–guest nanomaterial was dried in an oven at 60 °C for 12 h and under vacuum, for 2 h. The obtained material was denoted as CuL-NaBEA, where L represents the 9-methyladenine ligand.

2.2 Physical measurements

Total copper ion concentrations in cation exchange treatment were measured using a Varian Spectra AA-400, Atomic Absorption Spectrophotometer (AAS). The elemental analysis of carbon, hydrogen and nitrogen of the materials was carried out on a Leco CHNS-932 analyzer. Powder EPR spectra were carried out with a Bruker EMX spectrometer working at the X-band microwave frequencies (*ca.* 9.5 GHz) at room temperature. In order to correct possible deviations caused by electric charge of the samples, the C 1s line at 285.0 eV was taken as internal standard.[27,28] Phase analysis was performed by XRD using a Philips PW1710 diffractometer. Scans were

taken at room temperature in a 2θ range between 4 and 80°, using Cu-Kα radiation. The SEM micrographs were collected on a LEICA Cambridge S360 Scanning Microscope equipped with an EDS system. To avoid the surface charging, prior to the analysis the samples were coated with gold in vacuum, by using a Fisons Instruments SC502 sputter coater. Room-temperature Fourier transform infrared (FTIR) spectra of ligand solutions and of solid samples (in KBr pellets) were measured using a Bomem MB104 spectrometer in the range 4000–500 cm^{-1} by averaging 20 scans at a maximum resolution of 4 cm^{-1}. The electronic UV-visible absorption spectra of methyladenine ligand and residual solutions were collected in the range 600–200 nm in a Shimadzu UV/2501PC spectrophotometer using quartz cells at room temperature. Thermogravimetric analyses (TGA) of the samples were carried out in a TGA 50 Shimadzu instrument under a high purity helium flow (50 cm^3 min^{-1}). All samples were characterized between 25 and 600 °C with a heating rate of 6 °C min^{-1}.

3 Results and discussion

3.1 Preparation of host (NaBEA)–guest (Cu(II) complex) nanomaterial

Beta zeolite modified by trapping a copper complex into its framework was prepared by using an excess of the 9-methyladenine ligand (ligand : Cu(II) molar ratio 4 : 1) in liquid phase at pH 7.

In the complex, the coordination of the 9-methyladenine ligand with the copper ion can occur at N_1 and N_7 on the purine ring and at the N-amino nitrogen (N_{am}), bonded to C_6 carbon of the 6-membered ring (Scheme 2).

In 9-methyladenine, the separation between N_1 and N_9 is approximately 4.0 Å (Scheme 2), suggesting that this ligand can easily diffuse into the structure of beta zeolite, which is characterized by an open pore diameter of 7.6 Å.[20] Therefore, the copper(II)–methyladenine complex can be synthesized in beta zeolite.

The amount of copper in the ion-exchanged BEA before the immobilization is estimated by the chemical analysis of the residual solution after ion-exchange treatment. The amount of uncomplexed copper ions in residual solution was equal to 2.60×10^{-1} mmol, which means a copper loading on BEA of 1.13×10^{-1} mmol g^{-1} of zeolite. The residual Cu(II) content is very high, indicating that only 30% of the copper initially present (3.73×10^{-1} mmol) has been retained by cation exchange inside the zeolite (Cu/Al ~ 0.1). The potential for cation exchange is proportional to the Al-content of the zeolite and, therefore, is lower for NaBEA zeolite compared to a zeolite with lower Si/Al ratio such as zeolite NaY.[29]

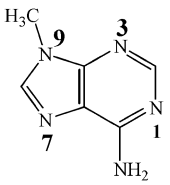

Scheme 2 Structure of the 9-methyladenine ligand.

The various steps of the *in situ* synthesis of the complex into BEA zeolite were monitored by a combination of characterization techniques. In particular, the residual solutions obtained from the immobilization process were analyzed before and after Soxhlet extraction by chemical analysis (CA), FTIR and UV-Vis spectroscopy. After Soxhlet extraction with ethanol, the CuL-NaBEA sample retained its initial grey colour. The electronic absorption spectrum of the methyladenine ligand exhibits two highly intense broad bands at λ_{max}(EtOH) = 210 and 260 nm due to π–π* transitions.[30,31] The presence of the methyladenine ligand in the residual solutions before Soxhlet extraction was evidenced by the appearance of the band at λ_{max}(EtOH) = 260 nm in the UV-Vis spectra, thus indicating that the excess ligand in the initial solutions, not adsorbed by the zeolite, was removed by filtration. FTIR also reveals the presence of bands due to the ligand, thus confirming the UV-Vis results. The FTIR spectrum of the 9-methyladenine ligand in KBr is characterized by the strong and medium bands appearing between ν_{max} = 1617 and 1300 cm^{-1}, attributed to skeletal vibrations of the purine ring, and by the typical free N–H stretching vibration at ν_{max} = 3273 cm^{-1} and N–H bending vibration at ν_{max} = 1679 cm^{-1} of the amino group on the 6-position of the ring.[30] After Soxhlet extraction, FTIR and UV-Vis analyses proved the presence of methyladenine ligand and of the complex in the extracting solvent. These results indicate that the Soxhlet extraction was able to remove the complex adsorbed on the external surface of the zeolite and the uncomplexed ligand.

3.2 Characterization of the host–guest nanomaterial

The CuL-NaBEA material was characterized by XRD and SEM analyses, spectroscopic methods (FTIR and EPR), chemical analysis (CA) and thermal analysis (TGA).

XRD powder patterns of the NaBEA and host–guest nanomaterial are presented in Fig. 1. All materials exhibited the typical pattern of highly crystalline beta zeolite with broad and sharp reflections.[32] No variation was observed in the

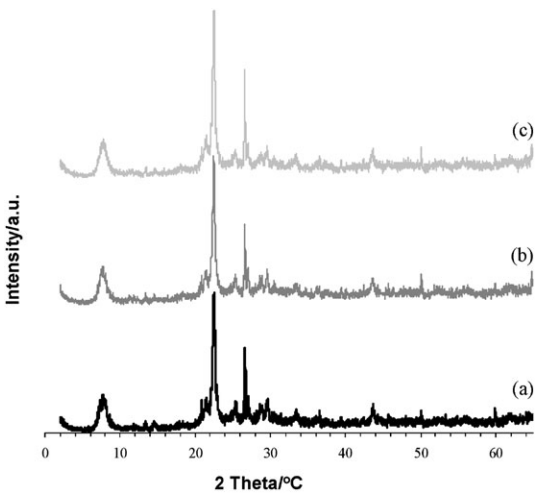

Fig. 1 XRD powder patterns of (a) NaBEA, (b) Cu-NaBEA and (c) CuL-NaBEA.

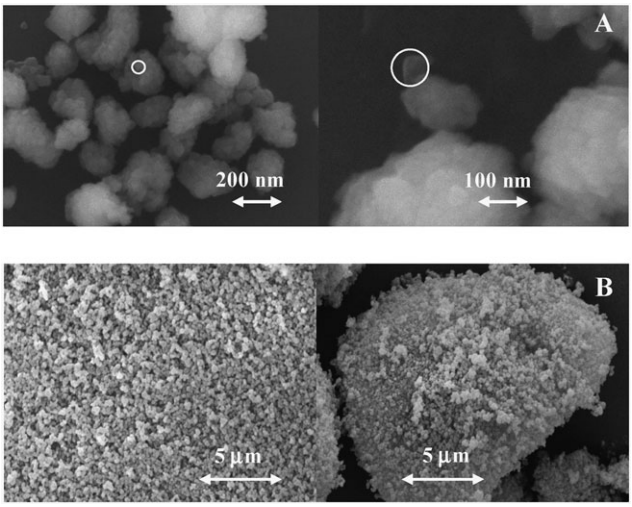

Fig. 2 Scanning electron micrography (SEM): (A) NaBEA with different resolutions. The circled area indicates a primary nanoparticles; (B) NaBEA (left) and CuL-NaBEA (right) at the same resolution.

characteristic peaks of zeolite after the introduction of the metal complex.

The morphology of the host–guest nanomaterial obtained before and after the immobilization process was determined by SEM analysis (Fig. 2).

From Fig. 2(A) two types of particles with different dimensions can be observed: (i) crystals of primary particles with a diameter of ~20–40 nm and (ii) aggregates of primary particles with a diameter of ~200–300 nm. The SEM micrographs of the parent and host–guest nanomaterial in Fig. 2(B) indicate that no changes occur in the BEA morphology and structure upon immobilization of the complex.

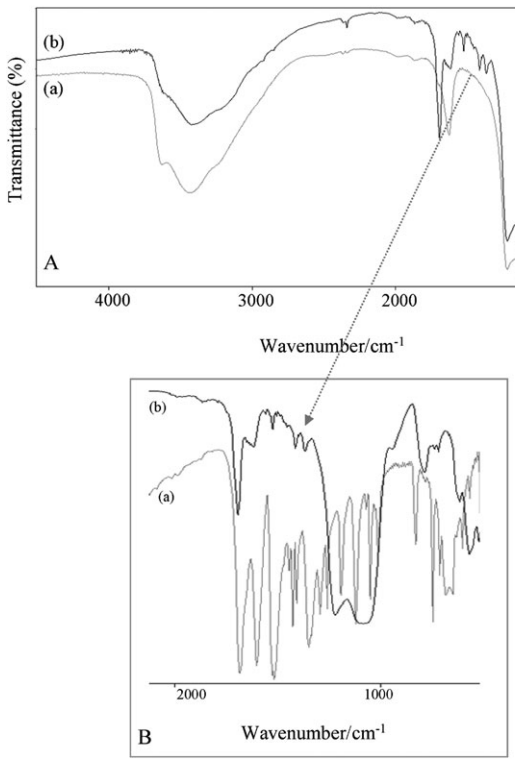

Fig. 3 (A) FTIR spectra in the range 4000–500 cm^{-1} of Cu-NaBEA (a) and CuL-NaBEA after Soxhlet extraction (b). (B) FTIR spectra in the range 2000–600 cm^{-1} of methyladenine ligand (a) and CuL-NaBEA after Soxhlet extraction (b).

Confirmation of the immobilization of the Cu(II) complex in Cu-exchanged NaBEA is provided by vibrational spectroscopy data. The infrared spectra in the range 4000–500 cm^{-1} (A) of the Cu–NaBEA (a) and CuL-NaBEA after Soxhlet extraction (b) and in the range 2000–600 cm^{-1} (B) of the methyladenine ligand (a) and of the CuL-NaBEA after Soxhlet extraction (b), are presented in Fig. 3.

The FTIR spectra of the Cu–NaBEA and host–guest nanomaterial are dominated by the strong bands assigned to the vibration of zeolite structure. The presence of physisorbed water is detected by the ν(O–H) stretching vibration at 3450 cm^{-1} and the δ(O–H) deformation band at 1640 cm^{-1}. In the former band, there is a shoulder band at around 3615 cm^{-1} assigned to OH in Si–(OH)–Al groups in the framework, which correspond to Brønsted acidity.[33] The large and broad peak at 1090 and 1060 cm^{-1} is due to asymmetric stretching vibration from O–Si–O,[34] while framework vibrations appear in the region 650–500 cm^{-1}.[29] No shift or broadening in the principal beta zeolite vibrations bands occur upon inclusion of the complex but for the δ(O–H) deformation band a shift from 1640 cm^{-1} to 1710 cm^{-1} is observed, suggesting that the inclusion of the complex in the zeolite structure provides possible host–guest interactions with OH groups of the zeolite.

In the CuL-NaBEA spectrum, the presence of the encaged complex can be detected by bands at ν_{max} = 1561, 1525, 1414 and 1347 cm^{-1}, typical of the purine ring, which appear shifted when compared with those of the free ligand. This suggests that the confinement in the void space of BEA zeolite causes a distortion of the complex structure. After the Soxhlet extraction from FTIR data (Fig. 3(A), curve b), the characteristic band of N–H stretching vibration at ν_{max} = 3273 cm^{-1} is not observed, suggesting the coordination of the copper ion with the methyladenine ligand and the absence of free ligand within the zeolitic matrix. The results indicate that the metal complex has been entrapped in BEA and also suggest the presence of host–guest interactions with the zeolite structure.

Chemical analysis was also carried out on the host–guest nanomaterial. The obtained results, together with the molar Si/Al and elemental analysis, are presented in Table 1.

The molar Si/Al ratio in CuL-NaBEA material did not change substantially upon immobilization of the guest, indicating that dealumination does not occur during the ion-exchange and immobilization procedure. The Cu/N ratio suggests the presence of one type of Cu/ligand complex with

Table 1 Chemical analysis results (wt%) of the host/guest nanomaterials

	Si/Al[a]	Cu[a]	C[b]	N[b]	Cu/N	Cu/C
NaBEA	8.80	—	—		—	—
CuL-NaBEA	3.04	0.52	4.21	2.72	0.19 (0.20)[c]	0.12 (0.17)[c]

[a] Bulk Si/Al ratio and copper loading on NaBEA determined by ICP-AES analysis. [b] Carbon and nitrogen from copper complex obtained by elemental analysis. [c] Values in parentheses refer to the theoretical ratio of Cu/N and Cu/C (w/w) in the copper complex.

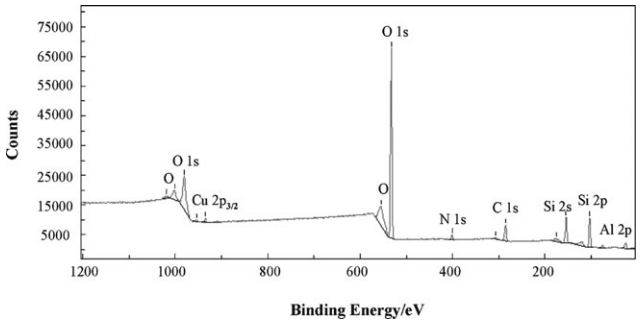

Fig. 4 High-resolution XPS spectrum of CuL-NaBEA.

a stoichiometry 1 : 1, while the Cu/C ratio indicates an excess of carbon ascribed to the organic solvents used in the processes.

We propose that copper(II) is coordinated with 9-methyladenine ligand by means of $N_{am}N_7$ (or $N_{am}N_1$) chelating groups (Scheme 2) while the other coordination sites are occupied by a water molecule and a zeolite framework oxygen.[9]

The presence of the guest in BEA zeolite was supported by XPS analysis. All samples revealed the presence of carbon, oxygen, sodium, silicon and aluminium in their XPS resolution spectra. In the CuL-NaBEA spectrum the presence of copper and nitrogen from the metal complex was detected (Fig. 4).

The bands typical of the Cu(II) complex, of fairly low intensity because of the low loading, were identified in the Cu $2p_{3/2}$ and N 1s region. The surface atomic content of the elements, obtained by the area of the relevant bands in the high resolution spectra, are presented in Table 2.

The bulk (Table 1) and the surface (Table 2) Si/Al atomic ratios on NaBEA and on host–guest nanomaterial were similar, confirming that the preparation method used in this work does not modify the zeolite structure. After the immobilization procedure, the amount of copper is lower at the surface (Table 2) than the bulk, which suggests that the complexes are preferentially located deep inside the large channels of BEA. The Cu/N ratio is the same as in the bulk, and is in agreement with the theoretical ratio for a 1 : 1 complex of Cu with methyladenine ligand.

Table 2 Surface elemental values (wt%) as calculated from areas under the XPS Si 2p, Al 2p, Na 1s, Cu 2p, N 1s, C 1s and O 1s bands

	Si	Al	Na	Cu	N	C	O	Si/Al	Cu/N
NaBEA	27.1	3.1	0.9	—	—	13.2	55.7	8.43	—
Cu-NaBEA	28.8	3.2	0.1	0.2	—	10.6	57.1	8.68	—
CuL-NaBEA	26.7	3.0	0.0	0.3	1.6	14.1	54.3	8.58	0.19 (0.2)[a]

[a] Values in parentheses refer to the theoretical ratio of Cu/N (w/w) in the copper complex.

Table 3 Curve fitting data of the XPS spectra in the Si 2p, Al 2p, Na 1s, Cu $2p_{3/2}$, N 1s, C 1s and O 1s bands

	Binding energy/eV						
	Si 2p	Al 2p	Na 1s	Cu $2p_{3/2}$	N 1s	C 1s	O 1s
NaBEA	104.0	75.4	1073.3	—	—	285.0	532.8
Cu-NaBEA	104.0	75.6	1071.8	932.6	—	285.0	532.7
							533.5
CuL-NaBEA	104.0	75.5	—	934.5	400.0	285.0	532.4
						287.0	533.5
						289.0	

The binding energies of the elements detected by XPS are summarised in Table 3. The most intense bands identified are due to the zeolite structure. In the Si 2p region a band at 104 eV is due to the tetrahedral Si atoms present in the zeolite, such as SiO_4 and terminal Si–OH groups; in the Al 2p region a band at 75.5 eV arises from the tetrahedral AlO_4 groups and a symmetrical large band at 532.4 eV from the O 1s region, is due to the oxygen atoms which are linked to the tetrahedral primary groups of the zeolite structure. Finally, a band in the region of Na 1s at 1072 eV, was also observed.

Bands due to the complex could be observed in the Cu $2p_{3/2}$, C 1s and N 1 s regions but with low intensity due to the low loading of the copper after ion exchange and following the formation of the immobilized complex. The medium binding energy values for Cu $2p_{3/2}$ are different before and after immobilization, which indicates the change in environment of the copper after the coordination with the methyladenine ligand. Before coordination the value is 932.6 eV and afterwards the medium binding energy value is 934.5 eV (Cu $2p_{3/2}$ of CuL-NaBEA), which confirms that the metal is in oxidation state two, in agreement with the copper coordination sphere of the free complex. This result shows that the host matrix environment does not affect the valence state of the metal atom of the complex.

The high-resolution C 1s spectra of CuL-NaBEA shows an asymmetric band centred at 285.0 eV that can be deconvoluted into three individual bands (Table 3).

The high intensity band at lower energy corresponds to the aromatic carbons from the 9-methyladenine ligand and the impurities from the preparation of CuL-NaBEA, in agreement with chemical analysis. The two other higher energy bands are assigned to carbons bounded to nitrogen atoms.[35] All samples exhibit an N 1s band centred at 400 eV, due to the contribution of the nitrogen atoms of the 9-methyladenine ligand.

Powder EPR spectra of Cu-NaBEA and CuL-NaBEA are presented in Fig. 5. All samples were cooled to 120 K for data acquisition to eliminate the effects of motional broadening that appear at room temperature.

The EPR spectrum of Cu-NaBEA (Fig. 5, curve a) exhibits four hyperfine features ($m_I = -3/2, -1/2, +1/2, +3/2$) in the low magnetic field region of the spectrum, characteristic of the copper nucleus with $I = 3/2$.[36] The CuL-NaBEA spectrum (Fig. 5, curve b) is qualitatively similar, but there are differences in the positions of the low-field hyperfine features as shown in the inset to the Fig. 5. The spectral broadening increases with increasing m_I value. The increase in broadening is due to the overlapping signals observed in the inset. These results indicate the presence of different copper species dispersed in the diamagnetic host, which suggests the presence of a small fraction of uncomplexed copper and of Cu^{2+} species coordinated with the methyladenine ligand in the first sphere of the complex.

The EPR parameters obtained are given in Table 4. The increase in $A_{\|}$ and the decrease in $g_{\|}$ values suggest an NNNN coordination around the Cu^{2+} ion.[9,37–39]

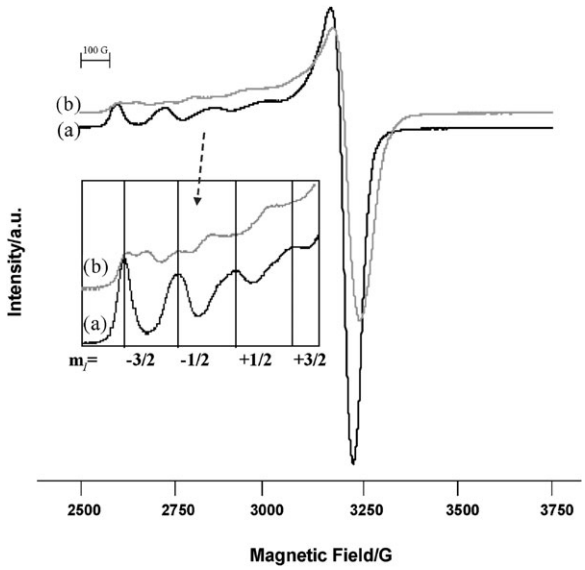

Fig. 5 EPR spectra of Cu-NaBEA (a) and CuL-NaBEA (b). Inset: Expansion of the hyperfine region between 2500 and 3200 G.

Table 4 EPR data of the host/guest nanomaterials

	$g_{\parallel}$	$g_{\perp}$	$10^4 A_{\parallel}/\mathrm{cm}^{-1}$
NaBEA	2.44	2.07	150
CuL-NaBEA	2.40	2.07	195

Thermogravimetric results (ESI,† Fig. S1) also give some information on the modifications of the BEA zeolite after the immobilization of the copper complex. The TG curve for the host NaBEA shows a significant weight loss near 150 °C, which can be attributed to the removal of intra-zeolite water, similar to that usually observed to other zeolites.[9] After immobilization of copper complex, two major stages of weight loss can be evidenced in a broad temperature range (*i.e.* 80–500 °C). The first stage occurs at 140 °C and is due to the contributions from the physisorbed water within the zeolite structure. For temperature nears 480 °C, the weight loss is associated with progressive decomposition of the immobilized complex.

4. Conclusion

The *in situ* synthesis of copper(II)–methyladenine complex in NaBEA zeolite has been achieved by free diffusion of the 9-methyladenine ligand derived from methyladenine through the zeolite pores exchanged with Cu(II) metal ion and with a ligand : Cu(II) molar ratio of 4 : 1.

By combining spectroscopic data with structural and morphological analysis it was possible to confirm that the copper(II)–methyladenine complex can be entrapped in the available cavities of beta zeolite, without damage of the original matrix or loss of its crystallinity. The framework structure of the BEA zeolite imposes steric restrictions to the formation of the complex. When compared with Y zeolite, which has supercages,[9] the amount of copper in BEA is lower and the methyladenine ligand has less space for coordination with copper ions inside the zeolite. For zeolite BEA, the geometry of the internal voids plays an important role in determining the molecular structure of the complexes and their amount inside the zeolite.

Acknowledgements

We thank Dr C. L. Remesar (GIQIMO, Santiago de Compostela University, Spain) for her kind help with the EPR measurements, Dr A. S. Azevedo (Departamento de Ciências da Terra of Universidade do Minho) for collecting the powder diffraction data and Dr C. Ribeiro, (Departamento de Ciências da Terra of Universidade do Minho) for performing chemical analyses. This work was supported by the Centro de Química (University of Minho, Portugal) and by Fundação para a Ciência e Tecnologia (FCT-Portugal), under programme POCTI-SFA-3-686.

References

1 M. E. Davis, *Nature*, 2002, **417**, 813.
2 A. Corma and H. Garcia, *Eur. J. Inorg. Chem.*, 2004, **6**, 1143.
3 P. P. Knops-Gerrits, D. E. DeVos, F. Thibault-Starzyk and P. A. Jacobs, *Nature*, 1994, **369**, 543.
4 D. E. DeVos, M. Dams, B. F. Sels and P. A. Jacobs, *Chem. Rev.*, 2002, **102**, 3615.
5 (*a*) *Chiral Catalyst Immobilization and Recycling*, ed. D. E. DeVos, I. F. K. Vankelecom and P. A. Jacobs, John Wiley and Sons, Weinheim, 2000; (*b*) D. E. DeVos, P. P. Knops-Gerrits, R. F. Parton, B. M. Weckhuysen, P. A. Jacobs and R. A. Schoonheydt, *J. Inclusion Phenom. Mol. Recognit. Chem.*, 1995, **21**, 185.
6 C. E. Song and S. Lee, *Chem. Rev.*, 2002, **102**, 3495.
7 A. Fuerte, M. Iglesias, F. Sanchez and A. Corma, *J. Mol. Catal. A: Chem.*, 2004, **21**, 227.
8 V. Ramaswamy, M. S. Kirshan and A. V. Ramaswamy, *J. Mol. Catal. A: Chem.*, 2002, **181**, 81.
9 N. Nunes, R. Amaro, F. Costa, E. Rombi, M. A. Carvalho, I. C. Neves and A. M. Fonseca, *Eur. J. Inorg. Chem.*, 2007, **12**, 1682.
10 M. Salavati-Niasari, *J. Mol. Catal. A: Chem.*, 2008, **283**, 120.
11 M. Maurya, A. K. Chandrakar and S. Chand, *J. Mol. Catal. A: Chem.*, 2007, **263**, 227.
12 M. Salavati-Niasari, *Inorg. Chem. Commun.*, 2006, **9**, 268.
13 H. Figueiredo, B. Silva, M. M. M. Raposo, A. M. Fonseca, I. C. Neves, C. Quintelas and T. Tavares, *Microporous Mesoporous Mater.*, 2008, **109**, 163.
14 J. G. Mesu, T. Visser, A. M. Beale, F. Soulimani and B. M. Weckhuysen, *Chem.–Eur. J.*, 2006, **12**, 7167.
15 P. K. Saha, B. Dutta, S. Jana, R. Bera, S. Saha, K. Okamoto and S. Koner, *Polyhedron*, 2007, **26**, 563.
16 M. Alvaro, B. Ferrer, H. Garcia and A. Sanjuan, *Tetrahedron*, 1999, **55**, 11895.
17 S. Ernst, H. Disteldrof and X. Yang, *Microporous Mesoporous Mater.*, 1998, **22**, 457.
18 (*a*) K. S. N. Reddy, M. J. Eapen, P. N. Joshi, S. P. Mirajkar and V. P. Shiralkar, *J. Inclusion Phenom. Mol. Recognit. Chem.*, 1994, **20**, 197; (*b*) S. Ernst, Y. Traa and U. Deeg, *Stud. Surf. Sci. Catal.*, 1994, **84**, 925; (*c*) R. C. Boggs, D. G. Howard, J. V. Smith and G. L. Klein, *Am. Mineral.*, 1993, **78**, 822.
19 (*a*) M. Alvaro, H. Garcia and M. N. Pillai, *PCT Int. Appl.*, WO 0311456, 2003; (*b*) T. Blasco, M. A. Camblor, A. Corma, P. Esteve, A. Martinez, C. Prieto and S. Valencia, *Chem. Commun.*, 1996, 2367; (*c*) M. A. Camblor, A. Corma and S. Valencia, *Chem. Commun.*, 1996, 2365.
20 Database of Zeolite Structures from the International Zeolite Association (IZA-SC)—www.iza-structure.org/databases/.
21 B.M. Weckhuysen, A. A. Verberckmoes, I. P. Vannijvel, J. A. Pelgrins, P. L. Buskens, P. A. Jacobs and R. A. Schoonheydt, *Angew. Chem., Int. Ed. Engl.*, 1996, **34**, 2652.
22 B. M. Weckhuysen, A. A. Verberckmoes, L. Fu and R. A. Schoonheydt, *J. Phys. Chem.*, 1996, **100**, 9456.

23 R. L. Wadlinger, G. T. Kerr and E. J. Rosinski, *US Pat*. 3308069, 1967.
24 A. H. M. Al-Shaar, R. K. Chambers, D. W. Gilmour, D. J. Lythgoe, I. McClenaghan and C. A. Ramsden, *J. Chem. Soc., Perkin Trans. 1*, 1992, 2789.
25 M. J. Alves, B. L. Booth, O. Kh. Al-Duaij, P. Eastwood, L. Nezhat, M. F. J. R. P. Proença and A. S. Ramos, *J. Chem. Res. (M)*, 1993, 2701.
26 R. K. Robins and H. H. Lin, *J. Am. Chem. Soc*., 1957, 490.
27 J. Y. Xie and P. M. A. Sherwood, *Chem. Mater*., 1990, **2**, 293.
28 J. F. Moulder, W. F. Strickle, P. E. Sobol and K. D. Bomben, in *Handbook of X-Ray Photoelectron Spectroscopy*, ed. J. Chastain, Perkin Elmer, Eden Prairie, MN, 1992.
29 A. Dyer, Zeolites and Ordered Mesoporous Materials: Progress and Prospects, *Stud. Surf. Sci. Catal*., 2005, **157**, 181.
30 G. Shaw, in *Comprehensive Heterocyclic Chemistry I*, ed. K. T. Potts, Pergamon Press, Oxford, 1984, vol. 5.
31 J. B. Lambert, H. F. Shurvell, D. A. Lightner and R. G. Cooks, in *Organic Structural Spectroscopy*, Prentice-Hall, NJ, 1998.
32 M. L. Kantam, B. P. C. Rao, B. M. Choudary, K. K. Rao, B. Sreedhar, Y. Iwasawa and T. Sasaki, *J. Mol. Catal. A: Chem*., 2006, **252**, 76.
33 M. A. Camblor, A. Corma and S. Valencia, *Microporous Mesoporous Mater*., 1998, **25**, 59.
34 C. Yang and Q. Xu, *J. Chem. Soc., Faraday Trans*., 1997, **93**, 1675.
35 A. P. Carvalho, C. Castanheira, B. Cardoso, J. Pires, A. R. Silva, C. Freire, B. Castro and M. B. Carvalho, *J. Mater. Chem*., 2004, **14**, 374.
36 P. J. Carl and S. Larsen, *J. Phys. Chem. B*, 2000, **104**, 6568.
37 P. S. Subramanian, E. Suresh and D. Srinivas, *Inorg. Chem*., 2000, **39**, 2053.
38 H. J. Scholl, J. Hutermann and M. S. Viezzoli, *Inorg. Chim. Acta*, 1998, **273**(1–2), 131.
39 A. Neves, C. N. Verani, M. A. Brito, I. Vencato, A. Mangrich, G. Oliva, D. D. H. F. Souza and A. A. Batista, *Inorg. Chim. Acta*, 1999, **290**(2), 207.